Published in final edited form as:
IEEE Trans Biomed Eng. 2010 January ; 57(1): 12–16. doi:10.1109/TBME.2009.2035103.

Real-Time 2-D Temperature Imaging Using Ultrasound

Dalong Liu [Student Member, IEEE] and
Department of Biomedical Engineering, University of Minnesota, Minneapolis, MN 55455 USA

Emad S. Ebbini [Senior Member, IEEE]*
Department of Electrical and Computer Engineering, University of Minnesota, Minneapolis, MN 55455 USA

Abstract

We have previously introduced methods for noninvasive estimation of temperature change using diagnostic ultrasound. The basic principle was validated both *in vitro* and *in vivo* by several groups worldwide. Some limitations remain, however, that have prevented these methods from being adopted in monitoring and guidance of minimally invasive thermal therapies, e.g., RF ablation and high-intensity-focused ultrasound (HIFU). In this letter, we present first results from a real-time system for 2-D imaging of temperature change using pulse-echo ultrasound. The front end of the system is a commercially available scanner equipped with a research interface, which allows the control of imaging sequence and access to the RF data in real time. A high-frame-rate 2-D RF acquisition mode, M2D, is used to capture the transients of tissue motion/deformations in response to pulsed HIFU. The M2D RF data is streamlined to the back end of the system, where a 2-D temperature imaging algorithm based on speckle tracking is implemented on a graphics processing unit. The real-time images of temperature change are computed on the same spatial and temporal grid of the M2D RF data, i.e., no decimation. Verification of the algorithm was performed by monitoring localized HIFU-induced heating of a tissue-mimicking elastography phantom. These results clearly demonstrate the repeatability and sensitivity of the algorithm. Furthermore, we present *in vitro* results demonstrating the possible use of this algorithm for imaging changes in tissue parameters due to HIFU-induced lesions. These results clearly demonstrate the value of the real-time data streaming and processing in monitoring, and guidance of minimally invasive thermotherapy.

Keywords

GPU; HIFU; image-guided surgery; therapeutic ultrasound

I. Introduction

Noninvasive temperature estimation continues to attract attention as a means of monitoring and guiding for minimally invasive thermotherapy. Currently, minimally invasive RF ablation is the most commonly used form of thermal therapy, but other techniques are being used or investigated. For example, high-intensity-focused ultrasound (HIFU) is being evaluated clinically as a form of noninvasive thermal therapy. Successful implementation of real-time noninvasive temperature estimation will be a boon for thermal therapy as it becomes less invasive and as the heating sources become more sophisticated.

*emad@ece.umn.edu..
liuxx293@umn.edu

Several methods have been proposed for temperature imaging using pulse-echo ultrasound, but echoshift estimation (using speckle tracking [1]-[3]) and spectral shift estimation (using high-resolution spectral estimation [4]) are most commonly used methods. The principle of measurement was validated experimentally by several groups in tissue and tissue-mimicking samples [5]-[7]. Both spectral and echoshift models for estimation of temperature change employed a linear model with a proportionality "constant" related to the temperature coefficient of the speed of sound, $\beta = (\partial c/\partial T)/c$, and the coefficient of thermal expansion α [8]. These methods, however, currently suffer from some limitations that have hindered their adoption in the clinic. These limitations stem from native tissue deformations (e.g., due to breathing and cardiac cycle) leading to echo and spectral shifts easily masking the (typically very small) temperature-induced shifts. Tissue strains due to fast switching of the heating source (as in pulsed HIFU or ON/OFF control of RF ablation) also produce artifacts due to undersampling of the tissue displacement fields at typical frame rates of 2-D ultrasound imaging.

In this letter, we present preliminary data to demonstrate a new temperature imaging mode employing M2D pulse-echo ultra-sound. A number of scan lines from the region of interest (ROI) are interrogated at high frame rate to capture the full thermal and mechanical transients of tissue motion/deformations in response to (pulsed) HIFU sources. This M2D mode is also suitable for capturing tissue motion and deformation within the ROI due to respiratory and cardiac cycles. We show temperature imaging results obtained by heating tissue-mimicking phantoms, as well as *in vitro* porcine heart. The results clearly demonstrate the advantages of ultrasound as a temperature imaging modality. Specifically, its high sensitivity to small ($\mathcal{O}(1\,^{\circ}\mathrm{C})$) temperature change, high spatial sampling, and high temporal resolution. In addition, the results demonstrate the feasibility of imaging tissue property change in HIFU-induced lesions based on the proposed method of imaging temperature change.

II. Methods

A. Temperature Estimation

The temperature change estimation method used in the current system is based on the thermal dependence of the ultrasound echo that accounts for two physical phenomena: local change in the speed of sound and thermal expansion of the medium due to changes in temperature. The speed of sound c is a function of temperature. In most tissue media around body temperature, c increases with temperature (see [9]). In fatty tissues, c decreases with increasing temperature [10]. In [1], we have described a temperature estimation algorithm based on speckle tracking relating changes in echo location to changes of tissue temperature. This approach was extended and fully described in [3]. It has been shown in [3] that

$$\Delta T(z) = \frac{c(T_0)}{2}\left[\frac{1}{\beta - \alpha}\right]\frac{\partial}{\partial z}(\delta t(z)) \tag{1}$$

where $\alpha = (\partial d(T)/\partial T)/d(T)$ is the linear coefficient of thermal expansion and $\beta = (\partial c(T)/\partial T)/c(T)$ is the thermal coefficient of the speed of sound. For a homogeneous medium, these parameters can be determined experimentally. Therefore, (1) suggests that temperature-change estimates can be obtained by first tracking the cumulative echo time-shift at each location, and then differentiating along the axial direction. This method was described and discussed in detail in [3], including the use of 2-D filtering for reduction of artifacts, e.g., thermal lens effect.

B. System Architecture

The system shown in Fig. 1 is used for applying pulsed HIFU, monitoring tissue response, and real-time processing of acquired data. A Sonix RP (Ultrasonix, Canada) ultrasound scanner

loaded with custom-designed program is used for high-frame-rate pulse-echo data collection. Collected data are then streamlined to a controller PC through Gigabit Ethernet for real-time data processing. The data processing computer can easily handle the intensive computations required by high-resolution (both spatial and temporal) speckle tracking and separable 2-D postfiltering by utilizing a many-core graphics processing unit (GPU; nVIDIA, Santa Clara, CA). The implementation of real-time data processing is further discussed in Section II-C.

The ultrasound scanner operates in B mode for image guidance and M2D mode for high-frame-rate data collection. The latter mode achieves high-frame-rate imaging by limiting the number of scan lines to the ROI, as defined by the user. M2D data is used for speckle tracking/ temperature estimation.

A Virtex2Pro (Digilent, Inc., WA) field-programmable gate array (FPGA) board is dedicated for HIFU source and synchronized frame trigger generation. The implementation allows an interference-free data collection by briefly silencing the HIFU generator while pulse-echo imaging is active.

C. Real-Time Data Processing

Temperature imaging relies on accurate estimation of incremental frame-to-frame time shifts, which are typically much smaller than RF-echo sampling period. The method that we have used is based on 2-D complex correlation of two subsequent frames of RF echo [3]. Our real-time data processing engine is based on a GTX285 GPU with 240 processing cores and designed to take full advantage of its highly parallel architecture. Fig. 2 shows a block diagram of the GPU-based implementation. Note that for each processing stage, fine-grained partition is performed for the algorithm in a data-independent manner so that all 240 processors are working efficiently on individual blocks of data.

To illustrate the computational efficiency of the GPU-based solution presented in this letter, Table I gives typical runtime values for the various components of the temperature imaging algorithm for a 4.1-s M2D-mode acquisition with 10 A lines per frame at 500 fps (see Section II-E). The table also shows typical specifications on the filters and windows used for the different algorithms.

D. Materials

Experiments were performed on elastography phantoms fabricated from gelatin, graphite, water, and glutaraldehyde in quantities suggested in [11]. The thermal properties were measured by slowly heating and cooling of the gel phantom in a water bath, as suggested in [3]. *In vitro* experiments were performed on fresh store-bought porcine heart tissue. All experiments were performed at room temperature.

E. Procedures

All heating experiments were performed using a 4-MHz HIFU transducer (Focus Surgery, Inc., IN) and monitored by the Sonix RP scanner. A linear array probe (LA14-5/38) was used for data collection at a frame rate of 500 fps in M2D mode by limiting the number of scan lines to 10 and the imaging range to 40 mm. A one-cycle transmit pulse with a center frequency of 9.5 MHz was used for imaging the tissue-mimicking phantom. The center frequency was set to 6.5 MHz when imaging the porcine heart tissue. The 9.5- and 6.5-MHz center frequencies were chosen to maximize the SNR of the RF data from the respective imaging targets.

1) Subtherapeutic Heating Procedure—The subtherapeutic heating procedur is as follows (see Fig. 3).

1) It starts with 400 ms tracking without application of heating beam to serve as baseline temperature.

2) With the tracking ON, heating beam starts to ramp up to full intensity in 200 ms and stays ON for another 1.5 s.

3) Another 2 s of tracking data are collected after the heating beam is turned off to capture the cooling phase.

2) Lesion-Formation Experiment Procedure—The lesion-formation experiment procedure is as follows.

1) Temperature profile with subtherapeutic level heating was measured to establish the tissue properties prior to lesion formation. The measurement was also performed multiple times to establish the repeatability and stability of tissue properties to the subtherapeutic level heating.

2) The HIFU transducer was driven with high power (50 W input electrical power) for 5 s to form a cigar-shaped (normal exposure) lesion at the HIFU focus.

3) Similar procedure as in 1) was performed 60 s after lesion formation. This sequence was repeated 18 times in approximately 1-min intervals to monitor transient behavior in tissue property change in response to therapeutic HIFU.

The tissue was dissected after the experiment and the presence of the HIFU-induced lesion was established by visual inspection. Based on our prior experience in forming HIFU lesions at different exposure levels, the lesions formed in this experiment were all normal, i.e., no signs of tissue damage due to boiling or violent cavitation [12].

III. Results and Discussion

A. System Validation With Elastography Phantom

The tissue-mimicking phantom was heated at a single spot using the HIFU transducer at subtherapeutic level using the procedure outlined earlier. The heating sequence was monitored using the Sonix RP in M2D mode. The HIFU transducer was driven at low power, i.e., in subtherapeutic mode, to produce small temperature rise (1 °C–3 °C) at the focus. The 4.1-s sequence was repeated multiple times at approximately 30-s intervals (to allow the temperature to go back to baseline.) Fig. 4 shows estimated temperature change profiles at the HIFU focus from eight repetitions of the subtherapeutic exposure. The mean value of peak temperature is 2.62 °C, while the standard deviation is 0.04 °C, which demonstrates the repeatability of the measurement. It also demonstrates the sensitivity of the method to small changes in target tissue temperature at frame rates and spatial resolution unmatched by other methods for temperature imaging, e.g., MRI.

B. Lesion Formation in Porcine Heart

Fig. 5 shows a gray-scale image of porcine heart tissue sample targeted by the HIFU transducer (at the dot location). The boxed area indicates the region where M2D mode RF data were acquired. This region is user-selectable using standard controls on the the Sonix RP console. Before the beginning of each sub-therapeutic heating procedure, the system operates in B-mode. When the procedure is initiated (from the console), the system switches to M2D mode and switches back to B-mode at the completion of the procedure.

Estimated temperature data resulting from heating the *in vitro* heart tissue are shown in Fig. 6. Since the data are 3-D (2-D + time), there are many ways of visualizing the data. We choose to display three projections based on a given coordinate (X, Z, and τ), where X stands for lateral

position, Z is the axial position, and τ is in the time direction. Projections shown in Fig. 6 are taken near the peak temperature in 3-D dataset. The temperature images shown demonstrate the spatial localization of the focal spot of the HIFU transducer, as can be clearly seen from the spatial and spatiotemporal representations. Note that the 2-D filtering of the estimated temperature change was minimal in this case to demonstrate the properties of the raw temperature images. For example, one can see the thermal lens effects that we reported in [3] in the region below the HIFU focus (as seen by the imaging probe). In addition, a large artifact due to surface motion near the top of the tissue sample (tissue-water interface) can also be seen. It is possible to eliminate or minimize these artifacts by using advanced signal processing methods, as was described in [13]. However, we use the raw temperature data to demonstrate the potential of this method, even with its current limitations.

To demonstrate the feasibility of tissue property measurement based on temperature imaging, we have run a sequence of 4.1-s subtherapeutic heating experiments (similar to the phantom experiments described previously) before and after lesion formation using a therapeutic HIFU shot, as described in Section IIE.2. Fig. 7 shows the maximum temperature change observed before and after the application of a therapeutic HIFU shot. Maximum temperature change in response to short subtherapeutic HIFU exposure is indicative of tissue absorption. One can see a clear separation between the measurements before and after lesion formation. One can also observe the transient nature of the change. In this particular case, it took approximately 4 min after lesion formation for the maximum change values to stabilize.

Fig. 8 shows the overlay of temperature profiles at the focal spot resulting from 9 experiments before and 15 experiments after HIFU application. Note that the first three datasets after HIFU application, as shown in Fig. 7, were not included for clarity. These results demonstrate that the clear separation in temperature change before and after lesion formation can be reliably measured within less than 1 s exposure at these power levels *in vitro*.

A one-to-one comparison of temperature profile before/after lesion formation is shown in Fig. 9. Several changes can be observed after the lesion was formed.

1) Higher temperature rise, which is primarily due to the increased absorption ratio that can be estimated by measuring the initial heating rate.

2) A faster mechanical response exhibited by the tissue upon terminating the HIFU sequence (see encircled region). This indicates an increase in tissue stiffness after lesion formation.

Note that the high frame rate is the key to capturing the mechanical response such as in 2). The fast transients would have been undersampled and unrecoverable if the data were acquired at lower frame rates. In fact, these transient responses were often missed when we collected data at normal frame rates (up to a 100 fps with a linear array probe), causing loss of tracking in temperature estimation in some cases.

IV. Conclusion And Future Works

We have presented the first real-time 2-D temperature-change imaging results from tissue media in response to subtherapeutic HIFU. A new data acquisition mode (M2D), together with high-performance computing implementation of the algorithm, were shown to produce highly sensitive (subdegree celsius) and repeatable images of temperature change in real time. Postprocessing techniques for improving the robustness of the method are currently being investigated, but some applications of the method are already possible: 1) The method can be used in the guidance of the HIFU beam and the characterization of the quality of the focus; 2) relative changes in tissue absorption can be measured (initial heating rate or maximum heating for short exposures) and, possibly, tissue perfusion (decay rate); and 3) relative changes in

tissue stiffness, which is known to occur upon protein coagulation. Therefore, real-time 2-D temperature imaging in M2D mode provides means for guiding HIFU beams at subtherapeutic levels before the application of the therapeutic pulse, improving the targeting and enhancing the chances of successful treatment. Furthermore, the method provides means for measuring changes in tissue-relevant properties (e.g., absorption and stiffness) at the lesion location, which may prove useful in the assessment of irreversible tissue damage.

Acknowledgments

Acknowledgment

The authors would like to thank Focus Surgery, Inc., for providing the therapeutic HIFU transducer used in the experiments described in this letter.

This work was supported in part by the National Institutes of Health under Grant EB009750.

REFERENCES

1. Seip R, VanBaren P, Simon C, Ebbini E. Non-invasive spatiotemporal temperature change estimation using diagnostic ultrasound. Proc. IEEE Ultrason. Symp 1995;1:1613–1616.
2. Maass-Moreno R, Damianou CA. Noninvasive temperature estimation in tissue via ultrasound echo shifts. Part I. Theoretical model. J. Acoust. Soc. Amer 1996;100:2514–2521. [PubMed: 8865654]
3. Simon C, VanBaren P, Ebbini ES. Two-dimensional temperature estimation using diagnostic ultrasound. IEEE Trans. Ultrason., Ferroelectr., Freq. Control Jul.;1998 45(no 4):989–1000. [PubMed: 18244253]
4. Seip R, Ebbini E. Non-invasive estimation of tissue temperature response to heating fields using diagnostic ultrasound. IEEE Trans. Biomed. Eng Aug.;1995 42(no 8):828–839. [PubMed: 7642197]
5. Miller NR, Bamber JC, Meany PM. Fundamental limitations of noninvasive temperature imaging by means of ultrasound echo strain estimation. Ultrasound Med. Biol 2002;28:1319–1333. [PubMed: 12467859]
6. Pernot M, Tanter M, Bercoff J, Waters K, Fink M. Temperature estimation using ultrasonic spatial compounding. IEEE Trans. Ultrason., Ferroelectr., Freq. Control May;2004 51(no 5):606–615. [PubMed: 15217237]
7. Souchon R, Bouchoux G, Maciejko E, Lafon C, Cathignol D, Bertrand M, Chapelon J-Y. Monitoring the formation of thermal lesions with heat-induced echo-strain imaging: A feasibility study. Ultrasound Med. Biol 2005;31:251–259. [PubMed: 15708465]
8. Amini AN, Ebbini ES, Georgiou T. Noninvasive estimation of tissue temperature via high-resolution spectral analysis techniques. IEEE Trans. Biomed. Eng Feb.;2005 52(no 2):221–228. [PubMed: 15709659]
9. Kinsler, LE.; Frey, AR. Fundamentals of Acoustics. 3rd ed.. Wiley; New York: 1982.
10. Rajagopalan, B.; Greenleaf, JF.; Thomas, PJ.; Johnson, SA.; Bahn, RC. Variation of acoustic speed with temperature in various excised human tissues studied by ultrasound computerized tomography. In: Linzer, M., editor. Ultrasonic Tissue Characterization II. Special Publication 525. US Government Printing Office; National Bureau of Standards, Washington, D.C.: 1979. p. 227-233.
11. Nightingale KR, Palmeri ML, Nightingale RW, Trahey GE. On the feasibility of remote palpation using acoustic radiation force. J. Acoust. Soc. Amer Jul.;2001 110:625–634. [PubMed: 11508987]
12. Ebbini ES, Yao H, Shrestha A. Dual-mode ultrasound arrays for image-guided surgery. Ultrason. Imag Apr.;2006 28:65–82.
13. Ebbini ES. Noninvasive two-dimensional temperature imaging for guidance of thermal therapy. Proc. Int. Symp. Biomed. Imag. (ISBI) 2006:884–887.

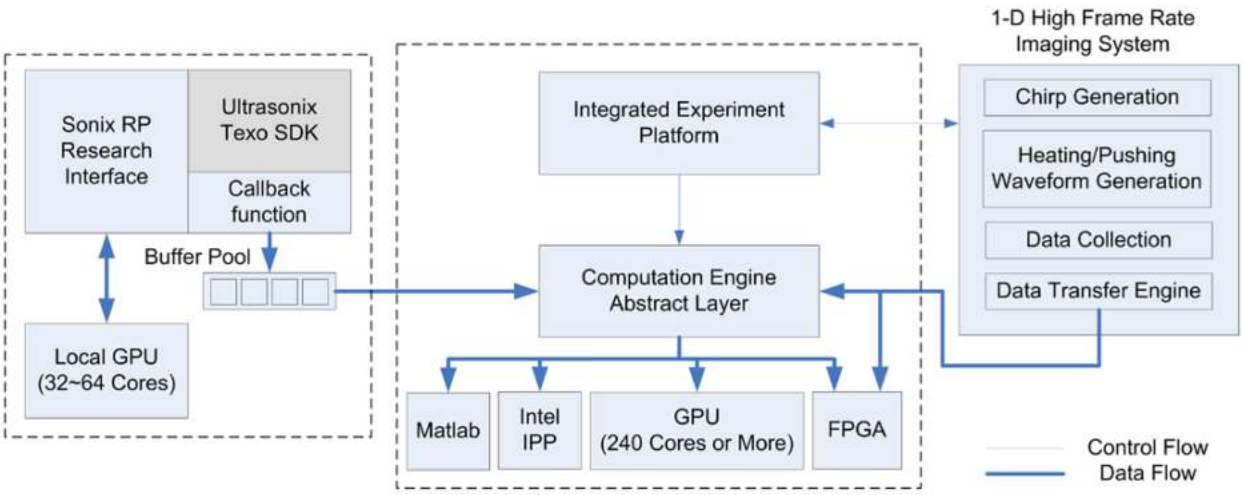

Fig. 1.
Block diagram of the imaging system, as it is currently implemented.

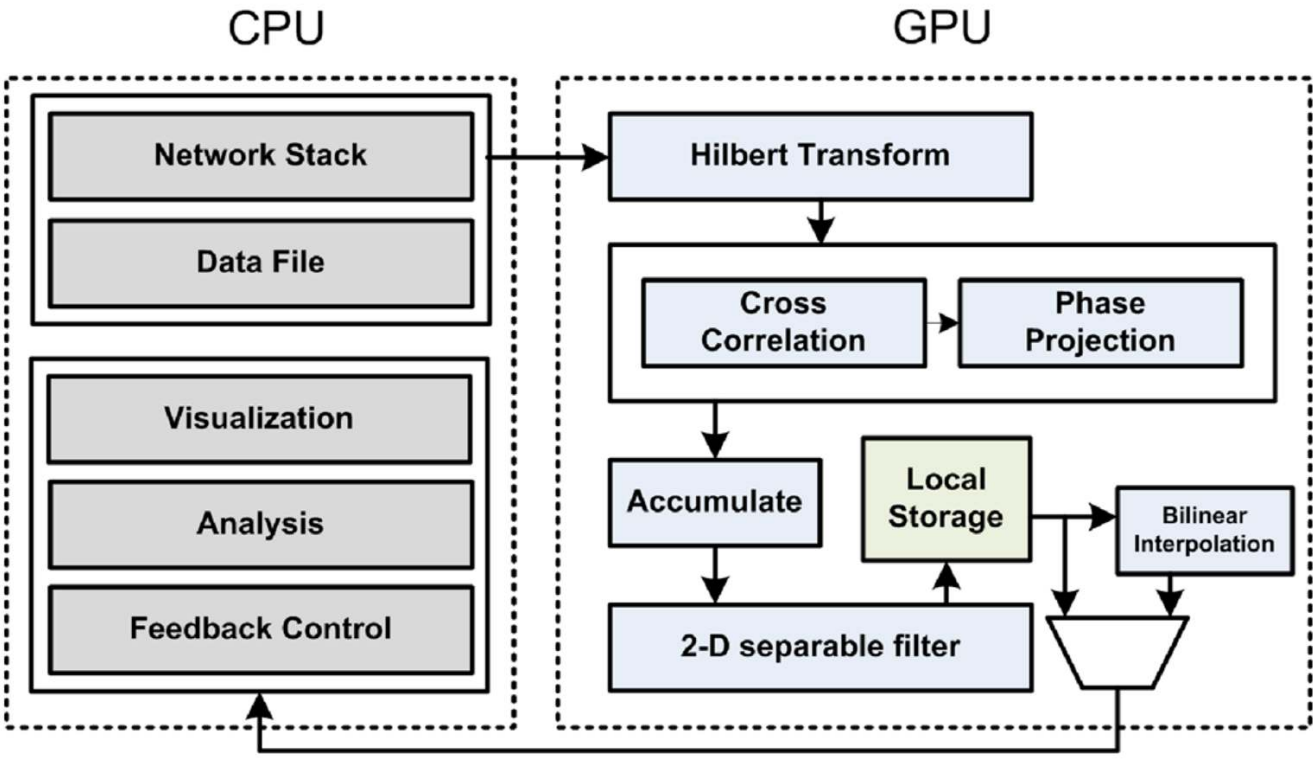

Fig. 2.
Block diagram of GPU implementation.

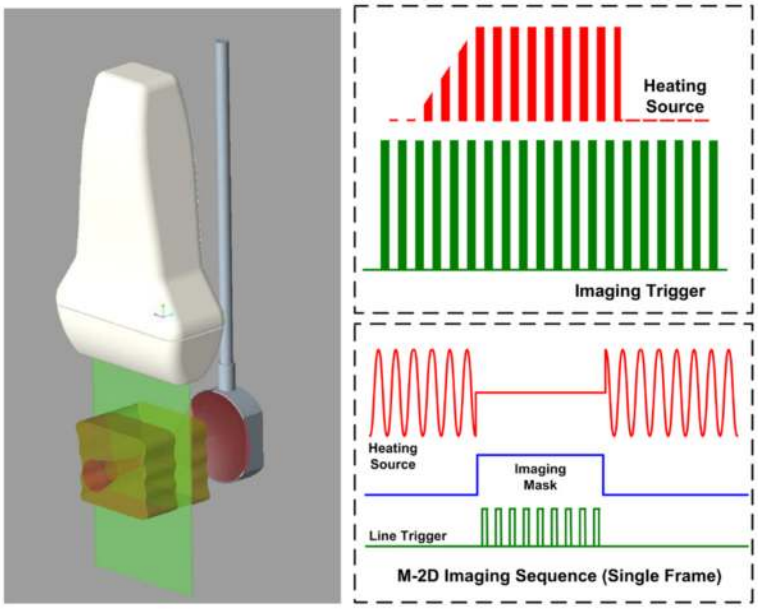

Fig. 3.
Experimental setup used in imaging localized temperature fields generated using a HIFU transducer. Note the imaging and therapy pulses are completely synchronized using the FPGA platform shown in Fig. 1.

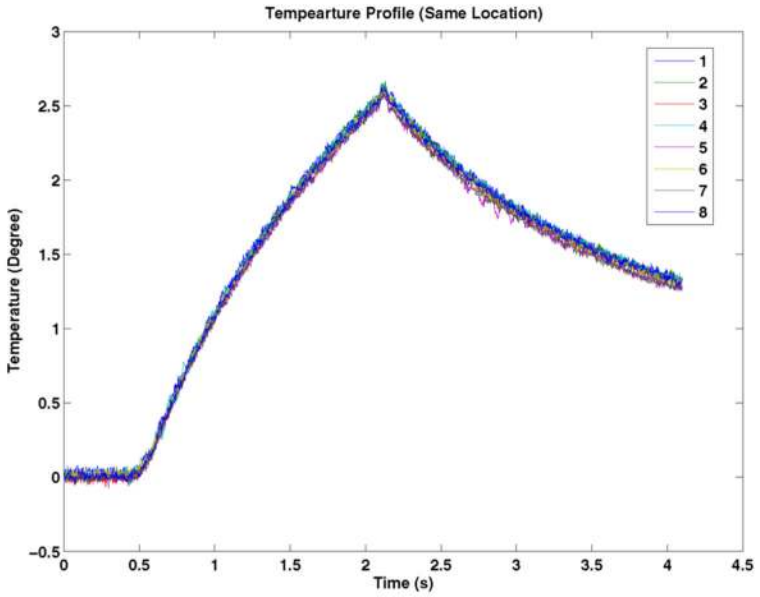

Fig. 4.
Temperature estimations for eight subtherapeutic heating experiments. All experiments were performed at the same location.

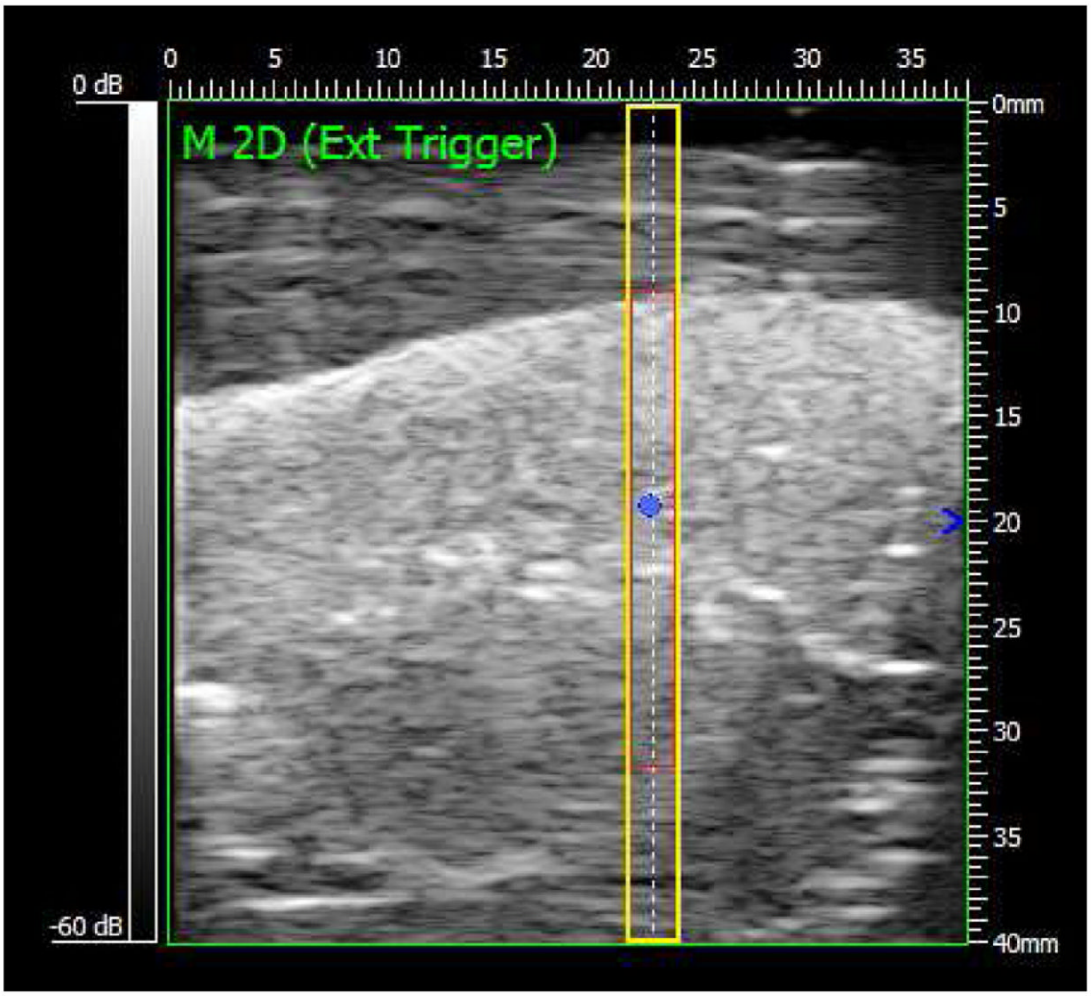

Fig. 5.
Guidance image for lesion formation experiment. The HIFU beam location is indicated by the heavy dot. The two overlapping boxes indicate M2D acquisition (the taller box) and the temperature processing zone (the shorter box). The extent of the temperature processing zone is determined by the SNR of the RF echoes from the M2D data.

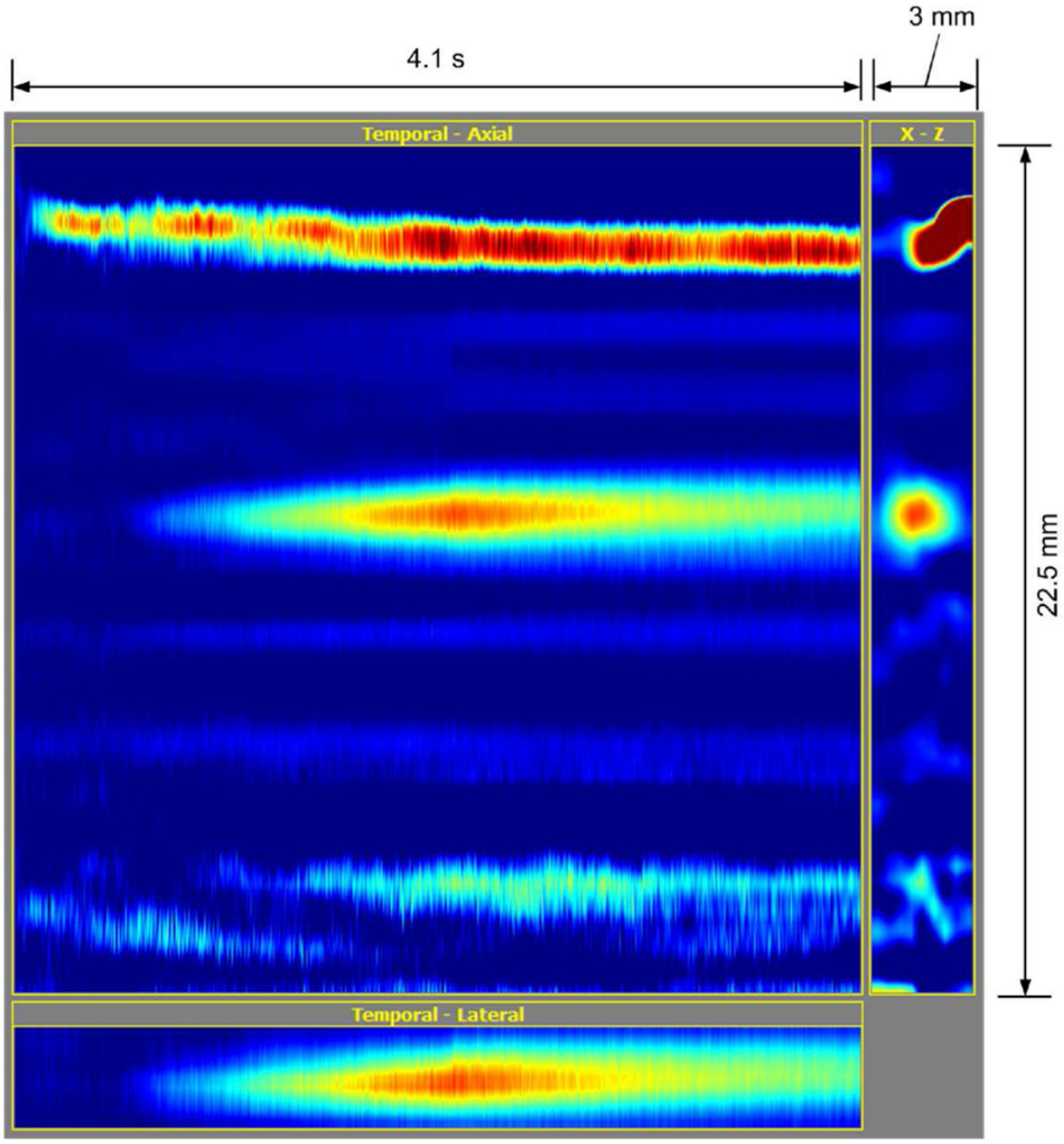

Fig. 6.
Example visualization of the 3-D (2-D + time) temperature data. The dataset is ten scan lines (3-mm) wide, 4.1-s duration at 500 fps. The upper right panel is an axial-lateral view just before switching OFF the HIFU focus (corresponding to the short box in Fig. 5). The upper left panel is an axial-temporal view from an A-line through the focal spot (indicated by the line and heavy dot in Fig. 5). The lower panel is a lateral-temporal view from a 3-mm lateral line within the heated region.

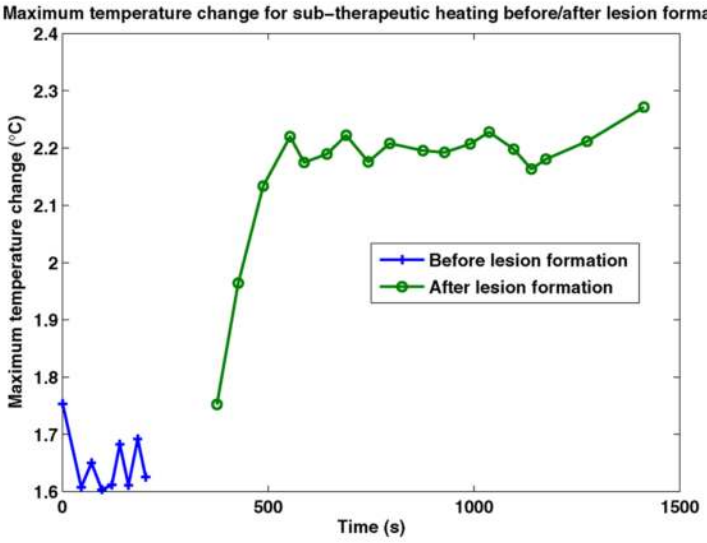

Fig. 7.
Maximum temperature change due to the application of 1.7-s subtherapeutic HIFU shots before and after the application of a 5-s therapeutic HIFU shot.

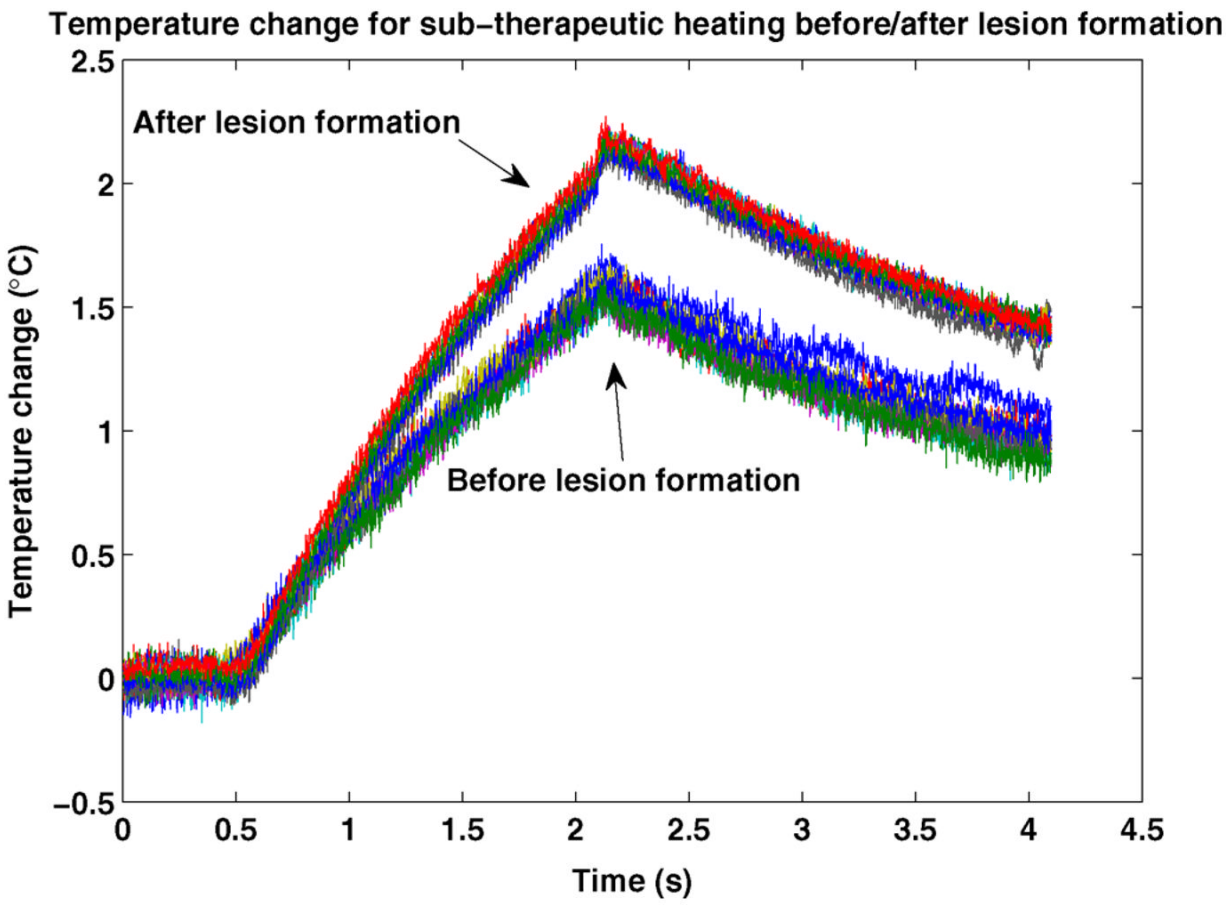

Fig. 8.
Temperature change before (nine datasets) and after (15 datasets) the HIFU application.

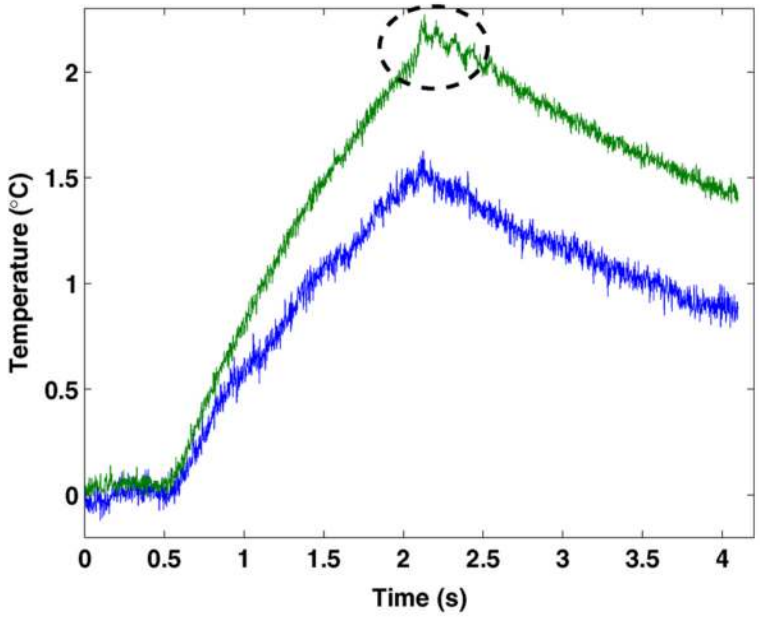

Fig. 9.
Temperature change before and after the HIFU application (one dataset).

TABLE I

Specifications and Run time for Signal Processing Components Used in Temperature Imaging

Algorithm	Specifications	Runtime
RF pre-filter	32 Taps	20.6 ms
Hilbert Transform	33 Taps	13.6 ms
Cross Correlation	33-sample window 97% overlap	106.4 ms
Phase Projection	3 A-lines	43.2 ms
Delay Accumulation		6.0 ms
Axial Differentiation	128 Taps	36.7 ms
Lateral MA Filter	4 Taps	10.4 ms